nature neuroscience

Genome-wide identification and characterization of functional neuronal activity–dependent enhancers

Athar N Malik[1–3,7], Thomas Vierbuchen[1,7], Martin Hemberg[4], Alex A Rubin[1], Emi Ling[1,5], Cameron H Couch[1], Hume Stroud[1], Ivo Spiegel[1], Kyle Kai-How Farh[1,6], David A Harmin[1] & Michael E Greenberg[1]

Experience-dependent gene transcription is required for nervous system development and function. However, the DNA regulatory elements that control this program of gene expression are not well defined. Here we characterize the enhancers that function across the genome to mediate activity-dependent transcription in mouse cortical neurons. We find that the subset of enhancers enriched for monomethylation of histone H3 Lys4 (H3K4me1) and binding of the transcriptional coactivator CREBBP (also called CBP) that shows increased acetylation of histone H3 Lys27 (H3K27ac) after membrane depolarization of cortical neurons functions to regulate activity-dependent transcription. A subset of these enhancers appears to require binding of FOS, which was previously thought to bind primarily to promoters. These findings suggest that FOS functions at enhancers to control activity-dependent gene programs that are critical for nervous system function and provide a resource of functional *cis*-regulatory elements that may give insight into the genetic variants that contribute to brain development and disease.

In the nervous system, sensory experience promotes both the refinement and maturation of synaptic connections and the subsequent modification of neural circuits during learning, memory and behavior[1–6]. Sensory experiences produce long-lasting changes in neuronal function in part through activity-dependent gene expression. In response to sensory input, synaptic activity leads to membrane depolarization of the postsynaptic neuron, triggering calcium influx through L-type voltage-gated calcium channels. This leads to the activation of a complex signaling network that alters the post-translational modification of transcription factors (MEF2, CREB and SRF), transcriptional cofactors (CBP) and chromatin modifiers (HDACs and MECP2), resulting in the transcription of early response genes[1,6]. Many early response genes encode transcription factors (FOS, FOSB, JUNB, EGR1, NR4A1 and NPAS4) that control the expression of late-response genes (for example, *Bdnf* and *Nptx2*) that regulate diverse aspects of nervous system development and function, including dendritic development, synapse maturation, synaptic plasticity, and learning and memory[2,7–9]. In total, several hundred neuronal activity–regulated genes have been identified, suggesting that activation of this gene expression program could broadly modify neuronal function. Furthermore, mutations in components of the neuronal activity–dependent transcriptional program have been linked to human cognitive disorders, including intellectual disability, autism spectrum disorders and psychiatric illness[10]. These findings have heightened interest in defining the functions of components of the activity-dependent signaling network in specific neuronal subtypes in the developing and mature nervous system.

There is still a striking gap in our understanding of how early response transcription factors such as FOS, C-JUN, NR4A1 and EGR1 function to promote the transcription of late-response genes[1,2,4]. Although these transcription factors are activated in virtually every mammalian cell in response to extracellular stimuli, it remains to be determined at a genome-wide level whether activity-induced transcription factors actually bind to gene promoters in neurons and, if so, how they facilitate transcriptional initiation. The best characterized of the early response transcription factors is FOS[11–13]. Reporter gene and DNA mobility shift assays have demonstrated that FOS binds as a heterodimer with JUN family members to the AP-1 motif (TGANTCA) within the promoters of stimulus-responsive genes and thereby stimulates late-response gene transcription[13]. However, it was not known where FOS complexes bind across the genome in stimulated neurons, if in fact FOS is a promoter-binding factor and the extent of the gene network activated by FOS in response to neuronal activity. In addition, the possibility that FOS binds to regulatory sequences other than promoters, such as enhancers, had not been broadly explored.

Enhancers are regulatory sequences that typically reside long distances from promoters yet are able to effectively boost gene transcription[14,15]. The advent of next-generation sequencing technologies such as chromatin immunoprecipitation paired with high-throughput sequencing (ChIP-seq) and genome-wide transcriptomics (RNA-seq) have facilitated the identification of enhancer sequences at a genome-wide level[16–18]. An emerging view is that enhancers bind transcription factors and enable spatiotemporal control of tissue-specific gene expression during development. In addition, enhancers are becoming increasingly appreciated

[1]Department of Neurobiology, Harvard Medical School, Boston, Massachusetts, USA. [2]MD-PhD Program, Harvard Medical School, Boston, Massachusetts, USA. [3]Division of Health Sciences and Technology, Harvard Medical School and Massachusetts Institute of Technology, Cambridge, Massachusetts, USA. [4]Department of Ophthalmology, Children's Hospital Boston, Harvard University, Boston, Massachusetts, USA. [5]Program in Biological and Biomedical Sciences, Harvard Medical School, Boston, Massachusetts, USA. [6]Broad Institute of MIT and Harvard, Cambridge, Massachusetts, USA. [7]These authors contributed equally to this work. Correspondence should be addressed to M.E.G. (michael_greenberg@hms.harvard.edu).

Received 4 April; accepted 14 August; published online 7 September 2014; doi:10.1038/nn.3808

as the sites of functional variation within the genome that contribute to human disease[19]. Thus, there is substantial interest in identifying enhancers that regulate nervous system development and function[20,21]. A key step toward this end will be to identify the enhancers that control activity-dependent gene transcription.

Chromatin and transcription factor signatures have been identified that enable the unbiased genome-wide detection of enhancers. For example, enhancers have been identified as sequences where H3K4me1 is enriched and transcriptional coactivators such as CBP or EP300 (also called p300) are bound[16,17]. Building on these findings, a recent study measured CBP binding before and after membrane depolarization in cortical neurons to identify neuronal activity–dependent enhancers[18]. Although nearly 12,000 H3K4me1-enriched genomic regions exhibited activity-dependent increases in CBP binding, this far exceeds the number of activity-regulated genes, suggesting that many of these enhancers might not function to promote activity-regulated transcription. Consistent with this possibility, several recent studies in non-neuronal cells have shown that only the subset of CBP- or p300-bound enhancers with H3K27ac are actively engaged in regulating transcription[22,23]. These data suggested that the presence of the H3K27ac signature might mark enhancers that are functionally engaged in regulating gene transcription.

It is not known which of the thousands of putative activity-regulated enhancers in neurons contribute to activity-dependent transcription or whether the H3K27ac mark is relevant to the function of these enhancers[24]. One possibility is that the subset of activity-regulated CBP binding sites that function as activity-dependent enhancers display an increase in H3K27ac in response to stimuli that induce activity-dependent gene transcription. If this increase in H3K27ac is correlated tightly with enhancer activation, it might be used to help identify the functionally relevant activity-dependent enhancers. Alternatively, a subset of CBP binding sites might have the H3K27ac signature before activation, facilitating subsequent events that are required for enhancer activation.

To distinguish between these possibilities, we performed ChIP-seq to assess the level of H3K27ac at enhancers before and after membrane depolarization of cultured cortical neurons. We found that neuronal activity induces an increase in H3K27ac at only a small subset of the ~12,000 CBP binding sites in neurons but that the presence of increased H3K27ac predicts with 100% accuracy the enhancers that are capable of stimulating activity-dependent gene transcription. Surprisingly, a large proportion of these activity-regulated enhancers bind FOS. We find that FOS binds almost exclusively to enhancers and mediates the neuronal response to activity by amplifying the transcription of a wide range of activity-regulated genes that control synaptic function.

In this study, we identify the subset of activity-regulated enhancers that control gene transcription in cultured cortical neurons and that appear to be active *in vivo* during the postnatal period when experience-dependent gene transcription regulates synaptic maturation. In addition, we find that FOS, a protein that was thought to bind primarily to gene promoters, functions almost exclusively at enhancers to mediate the neuronal transcriptional response to elevated levels of activity. As many of these FOS-bound enhancer elements are active in the developing postnatal brain, they are potentially sites of sequence variation that may underlie differences in human brain function and whose mutation could give rise to nervous system disorders.

RESULTS

Neuronal activity–regulated H3K27ac dynamics at enhancers

To clarify which of the ~12,000 previously characterized activity-regulated enhancers (i.e., those that exhibit enrichment of H3K4me1 and inducible binding of CBP, termed here CBP/H3K4me1-enriched enhancers) function to promote activity-dependent transcription, we used ChIP-seq to assess H3K27ac across the genome in mouse cortical neurons before and after exposure to elevated levels of KCl (55 mM). This treatment has been shown previously to lead to membrane depolarization and an influx of calcium into neurons through L-type voltage-sensitive calcium channels. The elevation in intracellular calcium then triggers activity-dependent gene transcription. A large number of studies have shown that membrane depolarization of cultured neurons with elevated levels of KCl is a valid way of identifying signaling network components that function in the intact brain to mediate the genomic response to a wide range of sensory stimuli[1,18].

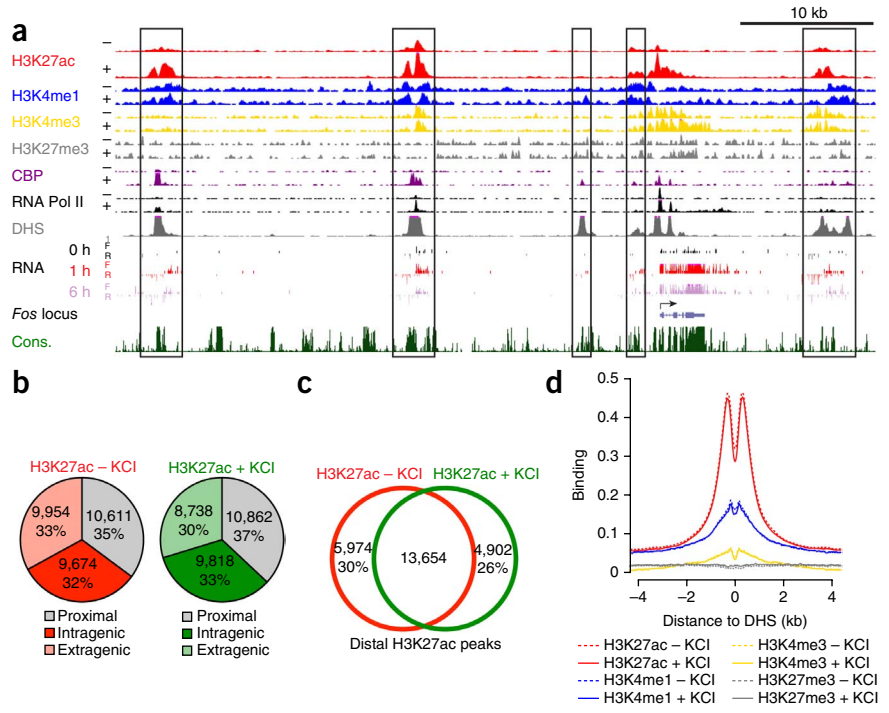

Figure 1 Genome-wide analysis of H3K27ac ChIP-seq peaks. (**a**) UCSC genome browser tracks of the *Fos* locus with data for indicated histone modifications, DNaseI hypersensitivity mapping from the P56 mouse cortex (generated by the mouse ENCODE project[27]). H3K4me1, H3K4me3, H3K27me3 RNA Pol II, CBP and RNA-seq (RNA; F, forward; R, reverse) tracks were generated previously[18]. Cons. indicates the Phastcons vertebrate conservation track. + and – indicate the presence and absence of KCl treatment, respectively. (**b**) Genomic distribution of H3K27ac peaks before (– KCl) and after (+ KCl) membrane depolarization. Peaks ±1 kb of a TSS are listed as proximal. (**c**) Overlap of gene-distal (>1 kb from a TSS) H3K27ac peaks before and after membrane depolarization. (**d**) Aggregate plot of H3K4me1, H3K4me3, H3K27ac and H3K27me3 signals before and after membrane depolarization centered at gene-distal DHSs enriched for H3K27ac.

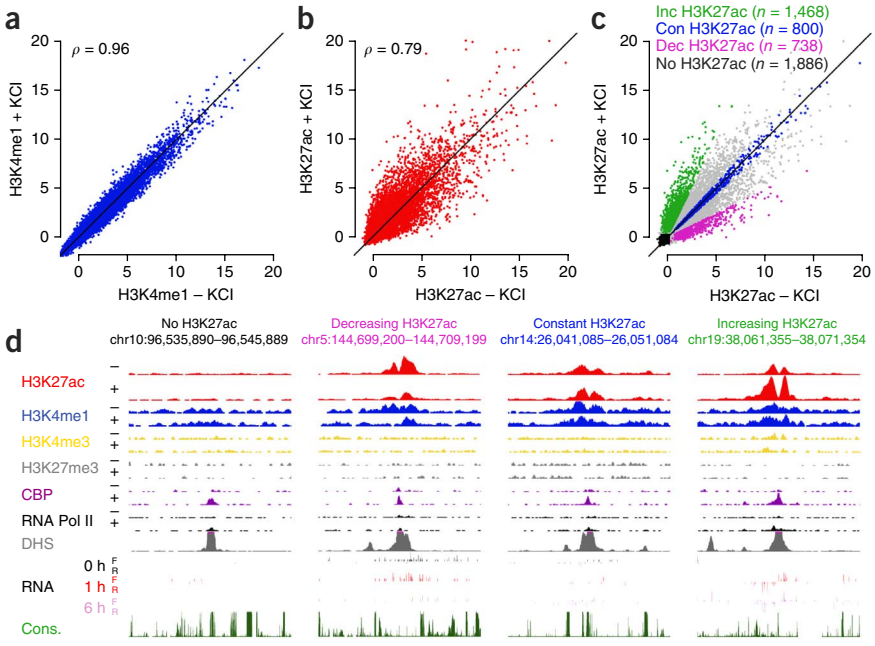

Figure 2 H3K27ac dynamics at activity-regulated enhancers. (**a**) H3K4me1 ChIP-seq signal at CBP/H3K4me1-enriched sites before and after 2 h of membrane depolarization by KCl ($\rho = 0.96$, Spearman's rank correlation coefficient). (**b**) H3K27ac ChIP-seq signal at CBP/H3K4me1-enriched sites before and after 2 h of membrane depolarization by KCl ($\rho = 0.79$, Spearman's rank correlation coefficient). (**c**) Classification of putative activity-regulated enhancers by distinct H3K27ac dynamics in response to neuronal activity (Online Methods). Inc, increasing; Con, constant; Dec, decreasing. (**d**) Representative loci demonstrating distinct H3K27ac dynamics at enhancers in response to neuronal activity. + and – indicate the presence and absence of KCl treatment, respectively.

We hypothesized that membrane depolarization might lead to the induction of H3K27ac at enhancers, which may be a key step in enhancer activation. To test this idea, we initially focused our attention on enhancers within the *Fos* locus. Activity-dependent induction of *Fos* transcription has been suggested to be mediated by five CBP/H3K4me1-enriched enhancers[18]. These putative *Fos* enhancers lie within 35 kb of the initiation site of *Fos* mRNA synthesis. We found that compared to untreated cells, exposure of cortical neurons to 55 mM KCl for 2 h led to a substantial increase in H3K27ac and CBP binding at the *Fos* promoter and at four of the five *Fos* enhancers described previously (**Fig. 1a**)[18]. This increase in H3K27ac correlated with a large increase in the production of *Fos* mRNA, raising the possibility that the activity-dependent increase in H3K27ac at the *Fos* enhancers might be required for enhancer activation and *Fos* transcription.

If the induction of H3K27ac at an enhancer is required for activity-dependent enhancer activation, then the induction of this modification at enhancers might be used to determine which among the thousands of putative enhancers are functionally engaged in driving activity-dependent transcription. To investigate this question, we first identified H3K27ac peaks genome wide before and after membrane depolarization. The H3K27ac ChIP-seq signal was highly reproducible between biological replicates (Spearman's $\rho = 0.91$ and $\rho = 0.94$ for unstimulated and membrane-depolarized replicates, respectively; **Supplementary Fig. 1a**,**b**). We filtered out peaks that were located within 1 kb of an annotated transcriptional start site (TSS), which likely represent promoters (**Fig. 1b**,**c**). Among these distal H3K27ac peaks, there were numerous peaks that we detected only after membrane depolarization ($n = 4{,}902$; **Fig. 1c**), suggesting that the genome-wide distribution of H3K27ac was modified by membrane depolarization. Both before and after membrane depolarization, these distal H3K27ac sites were enriched for the enhancer-associated

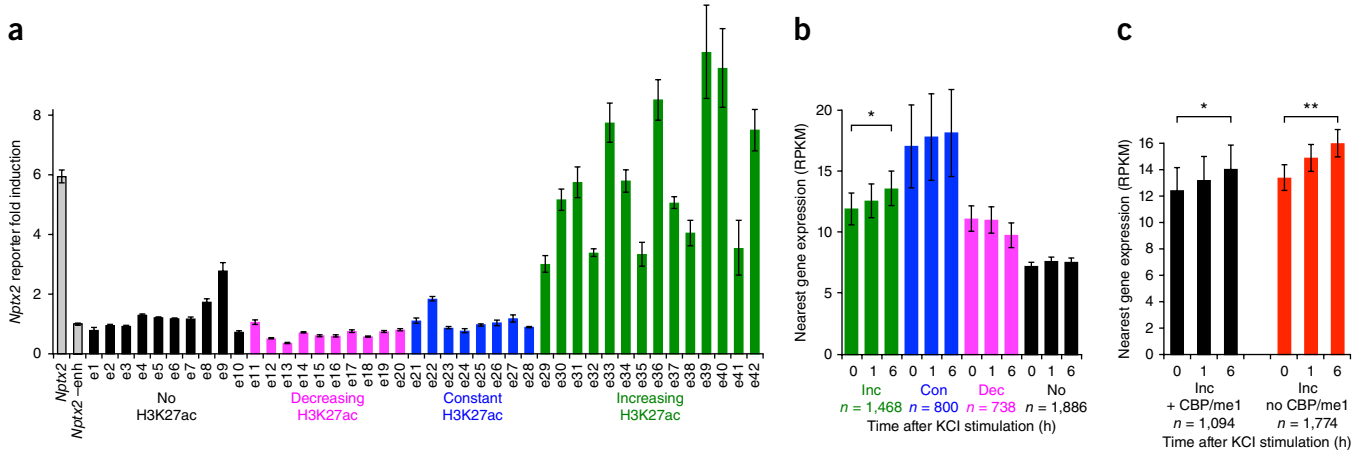

Figure 3 Functional analysis of enhancers with distinct H3K27ac dynamics. (**a**) Functional testing of enhancers from distinct H3K27ac classes in cultured cortical neurons at 7 days *in vitro* (DIV). All results are displayed as a fold increase over the *Nptx2* reporter backbone without the *Nptx2* enhancer (enh) element. Error bars represent the s.e.m. from three biological replicates with three technical replicates for each experiment. (**b**) Average expression of the nearest gene to elements from each class (measured by RNA-seq and shown as RPKM, reads per kb mapped). Gene expression analysis was performed after 0, 1 or 6 h of membrane depolarization by KCl (generated by Kim *et al.*[18]). $^{*}P = 7.83 \times 10^{-11}$, paired Wilcoxon signed rank test. The number of genes in each group is indicated below the *x* axis. Error bars represent the s.e.m. (**c**) Average expression of the nearest gene to enhancers with increasing H3K27ac with and without CBP/H3K4me1 (CBP/me1) enrichment ($^{*}P = 3.21 \times 10^{-8}$, $^{**}P < 2.2 \times 10^{-16}$, paired Wilcoxon signed rank test). Error bars represent the s.e.m.

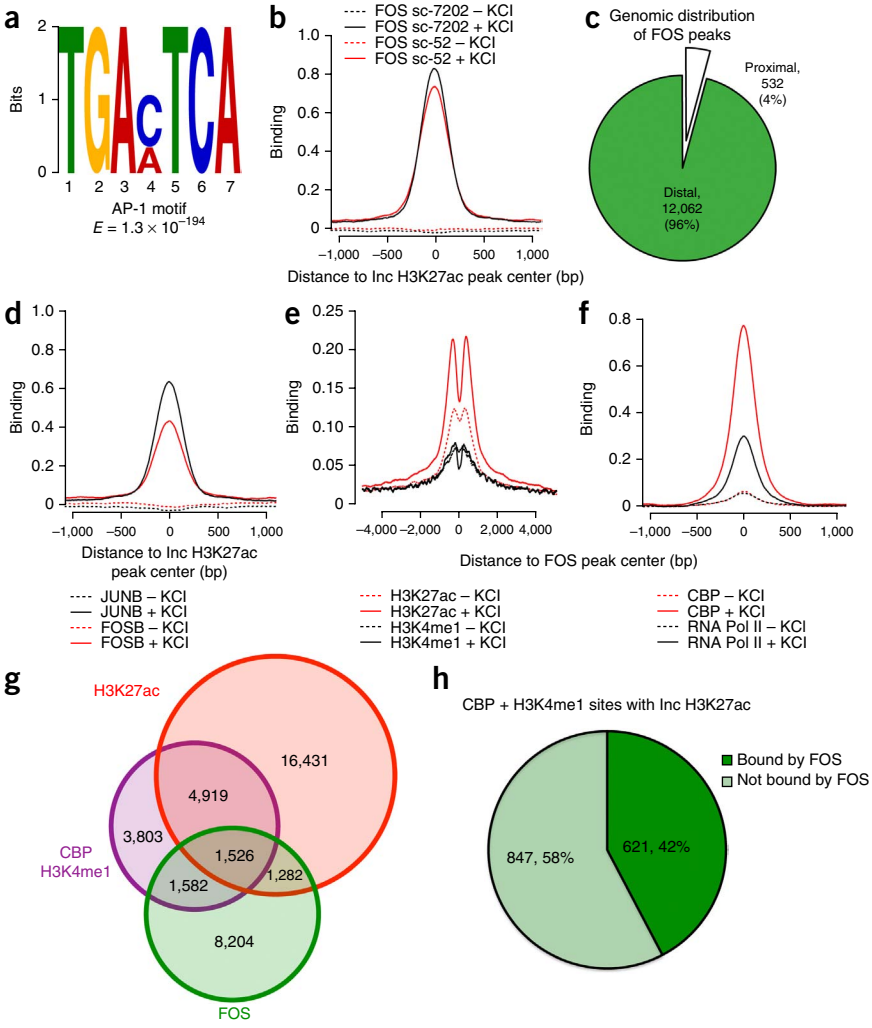

Figure 4 FOS binding is highly enriched at neuronal activity–regulated enhancers. (**a**) Position-weight matrix of the AP-1 site identified by a MEME *de novo* motif search performed with a search window of 150 bp from the center of the CBP peak within each activity-regulated enhancer. (**b**) Aggregate plots of ChIP-seq signals for FOS at activity-regulated enhancers. The signal from a ChIP-seq experiment performed with an additional FOS antibody (sc-7202) is also indicated. (**c**) Distribution of FOS peaks with respect to gene TSSs. Distal binding sites were defined as >1 kb from an NCBI annotated RefSeq TSS. (**d**) Aggregate plots of FOSB and JUNB binding at activity-regulated enhancers. (**e**) Aggregate plot of ChIP-seq signals for H3K4me1 and H3K27ac before and after membrane depolarization at FOS binding sites genome wide. (**f**) Aggregate plot of CBP binding and RNA Pol II binding before and after membrane depolarization at FOS binding sites genome wide. (**g**) Genome-wide overlap between H3K27ac peaks, CBP/H3K4me1-enriched sites and FOS peaks throughout the genome. (**h**) Fraction of increasing H3K27ac peaks bound by FOS.

histone modification H3K4me1 and had low levels of both H3K4me3 (associated with promoters) and H3K27me3 (associated with Polycomb-mediated gene silencing) (**Fig. 1d**). Notably, we observed that H3K27ac levels changed much more than H3K4me1 levels in response to neuronal activity at putative enhancers throughout the genome (Spearman's $\rho = 0.79$ and $\rho = 0.96$, respectively; **Fig. 2a**,**b** and **Supplementary Fig. 1c**,**d**), suggesting that changes in H3K27ac may reflect changes in enhancer function in response to neuronal activity. As a first step toward determining whether increased H3K27ac could be used to identify the CBP/H3K4me1-enriched sites across the genome that function as enhancers, we searched for CBP/H3K4me1-enriched sites with an increase in H3K27ac in response to membrane depolarization. Genome-wide quantification of H3K27ac levels at putative activity-regulated enhancers (CBP/H3K4me1-enriched sites >1 kb from an annotated TSS; Online Methods) revealed that a relatively small subset of these sites ($n = 1{,}468$, ~12%) exhibited at least a twofold increase in H3K27ac in response to membrane depolarization (**Fig. 2c**,**d**). Some putative activity-regulated enhancers exhibited a high level of H3K27ac before stimulation that remained unchanged after membrane depolarization, whereas other CBP binding sites displayed a low level of H3K27ac both before and after stimulation (**Fig. 2c**,**d**). We also identified sites that underwent a decrease in H3K27ac in response to membrane depolarization (**Fig. 2c**,**d**). Membrane depolarization–induced changes in the level of H3K27ac at gene-distal sites also occurred where we could not detect CBP/H3K4me1 enrichment (**Supplementary Fig. 1c–e**).

We divided each of the putative regulatory elements with CBP/H3K4me1 enrichment into four categories on the basis of their relative level of H3K27ac before and after membrane depolarization: those with increasing, constant, decreasing or no H3K27ac in response to stimulation (**Fig. 2c**,**d**). To determine whether the H3K27ac status of a putative activity-regulated enhancer can identify whether the enhancer is capable of stimulating activity-dependent transcription, we measured the ability of sites from each category to stimulate activity-dependent transcription. For this purpose, we developed a neuronal activity–regulated luciferase reporter gene in which 4 kb of the regulatory region of the activity-regulated gene encoding neuronal pentraxin 2 (*Nptx2*), including the *Nptx2* TSS, was cloned 5′ to the luciferase gene (Online Methods)[25]. The cloned *Nptx2* regulatory region includes an enhancer that is located ~3 kb upstream of the *Nptx2* TSS that we found to be critical for activity-dependent induction of reporter gene expression (**Fig. 3a**). To determine whether CBP/H3K4me1-enriched loci exhibiting activity-dependent increases in H3K27ac were capable of inducing activity-driven reporter gene transcription, we replaced the *Nptx2* upstream enhancer with 14 different enhancers with increasing H3K27ac enhancers and measured luciferase expression before and after membrane depolarization. Notably, we found that 100% (14/14) of these enhancers drove robust activity-dependent transcription of the luciferase reporter gene ($P = 2.44 \times 10^{-5}$, Student's *t* test, two tailed; **Fig. 3a** and **Supplementary Fig. 2a**). By contrast, CBP/H3K4me1-enriched loci that displayed constant levels of H3K27ac before and after stimulation or that exhibited no H3K27ac either before or after stimulation were not effective at inducing activity-dependent transcription of the luciferase reporter gene ($P = 0.206$ and $P = 0.422$, respectively, Student's *t* test, two tailed). Regulatory sequences with CBP/H3K4me1 enrichment and a reduction in H3K27ac after membrane depolarization led to a

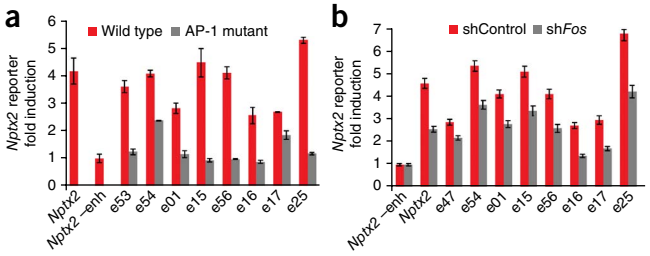

Figure 5 AP-1 transcription factors are required for the proper function of activity-regulated enhancers. (**a**) Effect of AP-1 site mutation on FOS-bound, activity-dependent enhancer function in the *Nptx2* reporter. AP-1 mutant enhancers (indicated on the *x* axis) have a single point mutation introduced into every AP-1 site within the enhancer that abrogates AP-1 complex binding. (**b**) Effect of *Fos* shRNA (sh*Fos*) co-transfection on activity-regulated enhancer activity compared to a control shRNA (shControl) plasmid (Online Methods). Error bars in **a** and **b** represent the s.e.m. for three biological replicates with three technical replicates for each experiment.

significant stimulus-dependent decrease in reporter gene transcription ($P = 0.0006$, Student's *t* test, two tailed; **Fig. 3a** and **Supplementary Fig. 2a**). For all enhancers tested, activity-regulated changes in H3K27ac were strongly correlated with changes in reporter gene expression ($R^2 = 0.73$). We confirmed these findings by placing selected enhancers from each group into two additional luciferase reporter constructs (containing either an SV40 or a minimal TATA-box promoter) to ensure that the activity-dependent transcriptional regulatory activity of these enhancers was not an artifact of the *Nptx2* reporter plasmid (**Supplementary Fig. 2**). We also tested whether sites with increasing H3K27ac but lacking CBP/H3K4me1 enrichment could function as activity-regulated enhancers in this assay. Enhancers with increasing H3K27ac but without CBP/H3K4me1 were significantly less active than those enriched for CBP/H3K4me1 ($P = 0.0003$, Student's *t* test, two tailed) (**Supplementary Fig. 3**). In total, these data suggest that the dynamic chromatin signature of increasing H3K27ac at CBP/H3K4me1-enriched enhancers is a specific and predictive signature of functional neuronal activity–dependent enhancers.

Although CBP/H3K4me1-enriched enhancers with increasing H3K27ac could activate reporter gene transcription in membrane-depolarized neurons, it remained possible that these enhancers might not function as activity-dependent enhancers in their normal genomic context. To address this issue, we investigated whether enhancers with increasing H3K27ac in response to neuronal activity are located near activity-regulated genes. For this analysis, we focused our attention on the four categories of CBP/H3K4me1-enriched sites described above, as well as enhancers with increasing H3K27ac in the absence of detectable CBP and/or H3K4me1 enrichment. We assigned regulatory regions from each of these groups of sites to the closest gene with detectable expression in neurons and quantified the expression of these genes using previously generated RNA-seq data[18]. Notably, we found that the expression levels of genes closest to these enhancers were highly correlated with the level of H3K27ac both before and after membrane depolarization (**Fig. 3b**). Enhancers with increased H3K27ac in response to neuronal activity were associated with activity-dependent increases in the expression of the nearest gene ($P = 7.83 \times 10^{-11}$, paired Wilcoxon signed rank test), and the expression levels of genes associated with enhancers that had constant H3K27ac were higher before and after depolarization than those of genes associated with loci with no H3K27ac. Moreover, the expression of genes nearest these two classes of activity-independent enhancers exhibited a less substantial increase in expression in response to neuronal activity than genes located near enhancers that displayed an activity-dependent increase in H3K27ac (**Fig. 3b**). In aggregate, the sites with increasing H3K27ac but without enrichment for CBP/H3K4me1 also exhibited a correlation with activity-dependent expression of the closest gene, suggesting that these sites also function as enhancers in the context of chromatin (**Fig. 3c**) despite their apparent lack of function in the luciferase reporter assays described above (**Supplementary Fig. 3**).

Taken together, these experiments indicate that the subset of CBP/H3K4me1-enriched sites that function as activity-regulated enhancers can be identified by the presence of an increase in H3K27ac in response to neuronal activity. In addition, sites with increasing H3K27ac but lacking CBP/H3K4me1 enrichment are also likely to be activity-dependent enhancers (given their correlation with activity-dependent gene expression); however, they exhibit significantly lower levels of enhancer function when measured in luciferase reporter assays. Of the 11,830 previously identified activity-regulated enhancers (H3K4me1-enriched sites with activity-inducible CBP binding),

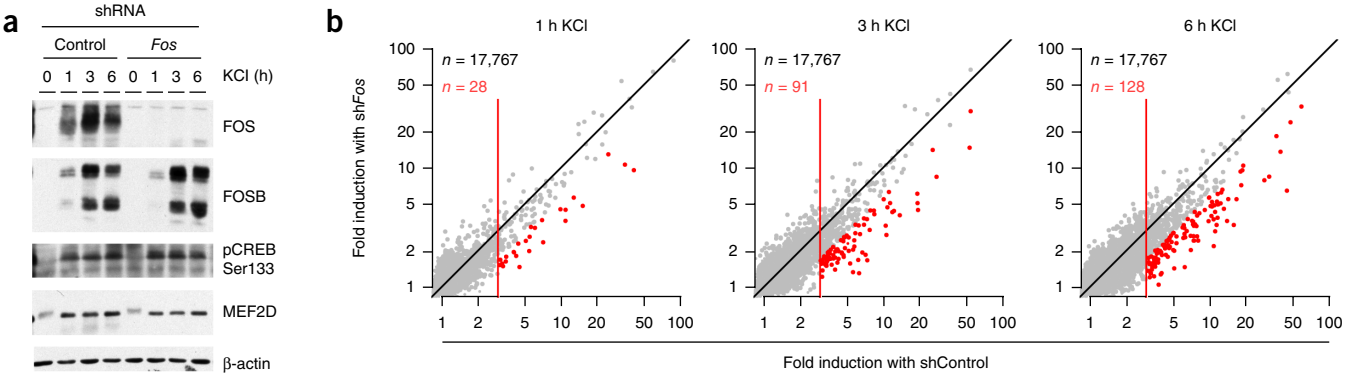

Figure 6 FOS activates an extensive gene program in neurons that regulates synaptic development and function. (**a**) Western blot for FOS, FOSB and proteins involved in activity-regulated signaling from cells expressing either shControl or sh*Fos* after 0, 1, 3 or 6 h of KCl stimulation. pCREB Ser133 indicates CREB phosphorylated at Ser133. This blot is representative of a total of three blots run for this set of experiments. (**b**) Quantification of microarray probe expression changes in cells expressing a lentiviral shRNA construct targeting FOS compared to a control shRNA targeting firefly luciferase. Neurons were treated with KCl for the indicated times (0, 1, 3 or 6 h), and gene expression was measured by microarray from biological replicate samples ($n = 2$ for each condition). The red lines indicate microarray probes induced by neuronal activity at least threefold at each of the three time points in the control condition. Red dots indicate activity-regulated microarray probes whose expression was reduced by at least 33%in the sh*Fos* condition compared to shControl. The number of total probesets at each time point and the activity-induced probes with 33% decreased expression in the *Fos* shRNA condition are listed on each scatterplot.

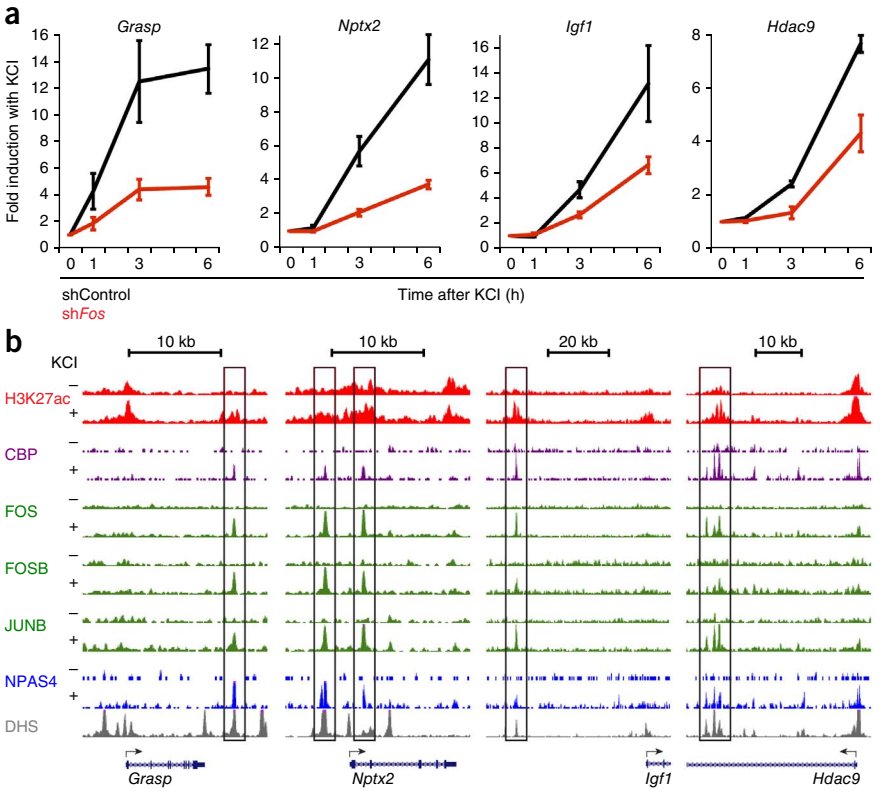

Figure 7 Integrated genomic analysis identifies direct targets of FOS. (**a**) Expression values measured by microarray of selected direct FOS target genes at each time point of KCl stimulation (error bars indicate the s.e.m., $n = 2$). (**b**) Genome browser tracks for each locus shown in **a** indicating enhancer-associated features and AP-1 transcription factor binding data. Putative enhancer elements are indicated by the boxed regions. The NPAS4 ChIP-seq data were generated previously[18].

1,468 displayed at least a twofold increase in H3K27ac signal and robustly drove expression of a reporter gene in luciferase assays and could thus be categorized as *bona fide* activity-regulated enhancers in cultured neurons (**Fig. 2c**). These loci will henceforth be referred to as activity-regulated enhancers.

In vivo function of activity-regulated enhancers

To test whether the activity-regulated enhancers identified in cultured cortical neurons function in the intact brain, we determined whether they overlap with DNaseI hypersensitive sites (DHSs) identified in the developing brain and adult mouse cortex by the mouse ENCODE project[26,27]. Sensitivity of chromatin to digestion by DNaseI allows for the identification of genomic regions that are bound by transcription factors and thus facilitates mapping of regulatory elements *in vivo*, including enhancers[28]. We found that ~99% of the activity-regulated enhancers identified in cultured neurons overlap with a DHS that has been mapped in published data sets in the mouse brain (embryonic day (E) 14.5 whole brain, E18.5 whole brain and adult cortex)[27]. This finding provides strong evidence that activity-regulated enhancers identified in cultured cortical neurons are also used during brain development and maturation. Notably, the degree of overlap between the activity-regulated enhancers and DHSs was greater in the adult cortex (955/1,468, 65.1%) than in the E14.5 whole brain (515/1,468, 35.1%) or the E18.5 whole brain (644/1,468, 43.9%). This observation suggests that many activity-regulated enhancers may not exhibit transcription factor binding until after birth, when sensory inputs increase the activity of cortical circuits and induce activity-regulated transcription in cortical neurons[3].

To further establish the *in vivo* relevance of the activity-regulated enhancers that we identified in cultured cortical neurons, we asked whether there was any overlap between our activity-regulated enhancers and those present in a recently published H3K27ac ChIP-seq data set of active forebrain enhancers identified across embryonic and postnatal brain development (E11.5, E14.5, E17.5, postnatal day (P) 0, P7, P21 and P56)[29]. Toward this end, we generated an aggregated data set of distal H3K27ac peaks from all of the stages of brain development ($n = 42{,}608$ peaks; Online Methods) and determined the overlap between the *in vivo* forebrain enhancers and the activity-regulated enhancers identified in cultured cortical neurons. This analysis revealed that a majority (74%) of the activity-regulated enhancers in membrane-depolarized cortical neurons overlap with H3K27ac enhancers identified in the forebrain.

Given that these experiments were performed using whole forebrain tissue from animals living in standard housing (no acute sensory stimulation), it is possible that H3K27ac ChIP-seq is not sufficiently sensitive to identify all of the neuronal activity–dependent enhancers that we detected in our *in vitro* cell culture experiments, as only a small fraction of cells in the intact cortex are engaged in activity-regulated transcription at any given time. However, taken together, these data indicate that the activity-dependent enhancers that we identified in cultured cortical neurons also function in the intact cortex during embryonic and postnatal brain development.

Sequence determinants of activity-regulated enhancers

To assess how activity-regulated enhancers function to regulate gene transcription, we performed *de novo* motif analysis to identify transcription factor binding motifs that are enriched in activity-regulated enhancers. The motif that was most significantly enriched among activity-regulated enhancers was the AP-1 motif (686 total AP-1 sites among 1,468 peaks of the activity-regulated enhancers; MEME motif score $E = 1.3 \times 10^{-194}$; **Fig. 4a** and **Supplementary Fig. 4a**)[30]. In parallel, we also determined the correlation between defined sequence motifs and membrane depolarization–induced changes in H3K27ac levels using an independent method that did not rely on the thresholded H3K27ac classes, which represent only the subset of CBP/H3K4me1-enriched sites that have the most distinct H3K27ac dynamics (Online Methods). This analysis identified three motifs having the highest correlations with increasing H3K27ac at enhancers: the AP-1 motif (average 1.41-fold change in H3K27ac ChIP signal with depolarization, $n = 3{,}962$ enhancers), the CREB motif (1.75-fold change, $n = 175$ enhancers) and the MEF2 motif (1.08-fold change, $n = 2{,}946$ enhancers). In addition, the E-box motif (0.87-fold change, $n = 5{,}011$ enhancers) was correlated with a decrease in H3K27ac signal in response to depolarization (**Supplementary Table 1**).

The transcription factor complex that binds preferentially to AP-1 sites consists of heterodimers of FOS- and JUN-family proteins, several of which (FOS, FOSB and JUNB) are robustly induced by

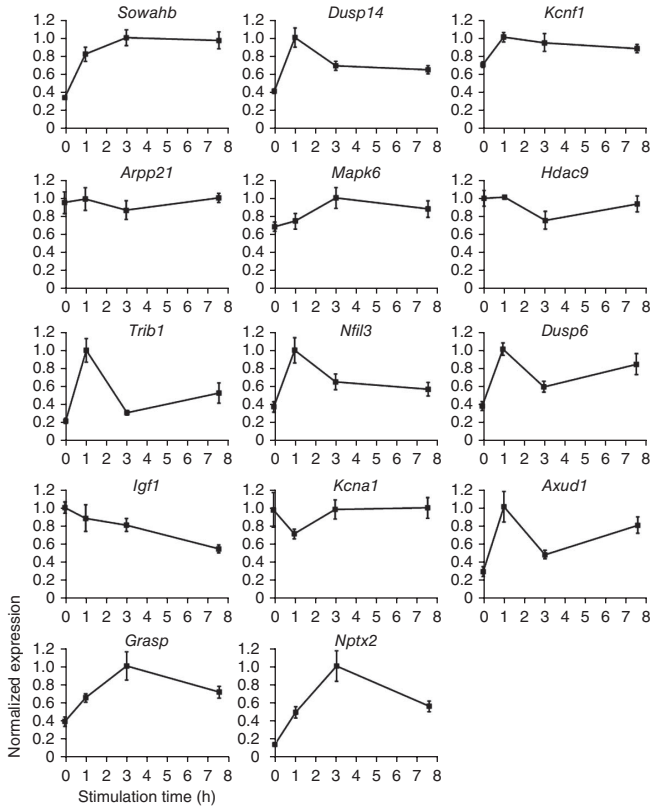

Figure 8 Expression of FOS direct target genes in mouse visual cortex. The expression of each indicated direct FOS target gene in the primary visual cortex was measured by qRT-PCR. Seven-week-old mice were dark housed for 1 week and exposed to light for the indicated time periods. Measured expression levels for each gene were normalized to the time point with the highest level of expression. Error bars indicate the s.e.m. from four animals.

neuronal activity[4]. Although JUN family members, but not FOS family members, can homodimerize, FOS-JUN heterodimers form preferentially when FOS family members are present, as is the case when neurons are exposed to sensory stimuli[13]. Because the prevailing view is that FOS–JUN complexes bind AP-1 sites within the promoters of late-response genes in response to extracellular stimuli, we were surprised to find that the AP-1 motif is so frequently present in activity-regulated enhancers. It had not previously been considered that FOS- or JUN-family heterodimers might function primarily at enhancers in neurons.

FOS binding at neuronal activity–inducible enhancers

Given the enrichment of the AP-1 motif within activity-dependent enhancers, we used ChIP-seq to determine whether FOS binds to these enhancers. We left cortical neurons unstimulated or exposed them to elevated levels of KCl for 2 h to achieve maximal induction of FOS protein. Under these conditions, we detected 12,594 FOS binding sites that were reproducibly detected across multiple experiments (**Fig. 4b**,**c**) and that were specific for the FOS protein based on ChIP-seq experiments with *Fos* short hairpin RNA (shRNA) (**Supplementary Fig. 5a**,**b** and Online Methods). Among these 12,594 FOS peaks, 80.3% contained an AP-1 motif, further suggesting that these sites were bound by FOS. ChIP-seq using antibodies to JUNB and FOSB revealed enrichment for inducible binding of these additional AP-1 transcription factors at FOS binding sites, confirming that FOS-JUN heterodimers likely bind to activity-regulated enhancers (**Fig. 4d**). We note that only a fraction of the activity-regulated enhancers shown in **Figure 2c** (the increasing H3K27ac group) are bound by FOS (621/1,468, 42%), suggesting that FOS binding alone does not determine whether an enhancer functions in an activity-dependent manner (**Fig. 4g**,**h**).

Surprisingly, an analysis of the localization of FOS binding sites across the genome indicated that FOS is bound predominantly to gene-distal sites, with the overwhelming majority located greater than 1 kb from an annotated TSS (96% of FOS binding sites; **Fig. 4c**). Furthermore, we found that in membrane-depolarized neurons, FOS binding sites are enriched for previously documented features of enhancers (H3K4me1, H3K27ac, CBP binding and RNA polymerase II (RNA Pol II) binding), suggesting that in cultured cortical neurons, activity-inducible AP-1 transcription factors bind predominantly to enhancers (**Fig. 4e**–**g**). In this respect, FOS binding differs from that of most other transcription factors, which have a less marked bias toward enhancer binding[31]. This observation could suggest that FOS functions in a specialized manner at enhancers to promote gene transcription in response to extracellular stimuli.

Given that FOS peaks at activity-dependent enhancers represent a relatively small fraction of all FOS peaks, we next sought to determine whether all or a subset of distal genomic sites bound by FOS have activity-regulated enhancer function. To accomplish this, we selected FOS-bound, gene-distal sites with different levels of CBP binding and H3K27ac enrichment, cloned these elements into the *Nptx2* reporter construct and tested their ability to function as activity-regulated enhancers. Consistent with our previous data (**Fig. 3a**), we found that only FOS binding sites that exhibit both CBP binding and increasing H3K27ac in response to neuronal activity drive activity-dependent reporter expression (**Supplementary Fig. 3a**). At the genome-wide level, we detected FOS binding at CBP/H3K4me1-enriched enhancers that displayed each of the changes in H3K27ac behavior described above; however, enhancers that displayed an increase in H3K27ac after membrane depolarization exhibited the highest level of FOS binding (42% bound; **Fig. 4h** and **Supplementary Fig. 6b**–**d**). We also observed FOS binding at sites with increasing H3K27ac but no CBP/H3K4me1 enrichment (**Supplementary Fig. 6e**). In total, these data suggest that the functionally active FOS-bound enhancers in membrane-depolarized neurons are the gene-distal FOS binding sites that are also bound by CBP/H3K4me1 and exhibit an increase in H3K27ac in response to membrane depolarization. It is likely that these FOS enhancers are also functionally active in the intact cortex, given that 64.4% of the FOS enhancers that we identified in membrane-depolarized cortical neurons are also enriched for H3K27ac in the forebrain *in vivo*.

Having shown that FOS binds to activity-regulated enhancers, we next tested whether FOS binding to these enhancers is required for enhancer activity. Toward this end, we tested eight different activity-inducible enhancers that exhibited high levels of FOS binding for their ability to drive activity-dependent expression of the *Nptx2* promoter luciferase reporter gene. We then compared the levels of induction by each enhancer with those of an identical enhancer in which each of the AP-1 sites was mutated by a single base pair to disrupt FOS binding (Online Methods). Whereas all eight wild-type enhancers could confer activity-dependent luciferase expression when cloned into the reporter gene, mutation of the FOS binding sites led to markedly reduced reporter gene transcription in each case, often to the level exhibited by the reporter gene in the absence of the enhancer (**Fig. 5a**). This result suggests that FOS binding is required for the

activity-dependent function of each of these enhancers. In further support of this conclusion, we found that the ability of each of the activity-dependent, FOS-bound enhancers to promote activity-dependent reporter gene expression was diminished by co-transfection with an shRNA that targets *Fos* compared to a control shRNA (**Fig. 5b**). Taken together, these findings suggest a model in which *Fos* expression is induced in response to neuronal activity, FOS together with a JUN family member (for example, JUNB) binds to enhancer sequences throughout the genome, and the subset of these enhancers that exhibit CBP/H3K4me1 enrichment and increasing H3K27ac then function to promote activity-dependent gene expression. The fact that a subtle mutation in the FOS binding site in an enhancer can have a marked effect on reporter gene transcription suggests that when similar mutations occur in endogenous activity–regulated enhancers, they may have substantial effects on sensory stimulus–dependent gene transcription.

Identification of FOS target genes in neurons

The finding that FOS controls enhancer activity across the neuronal genome suggests that FOS likely regulates a large number of activity-dependent genes that are important for nervous system development and function. However, although the induction of *Fos* in the brain has been studied extensively for several decades, so far there has been no attempt to identify the targets of FOS at a genome-wide level, and it is not known how many genes FOS activates in a given cell. To identify potential FOS target genes, we performed microarray analysis on RNA obtained from mouse cortical neurons infected with lentivirus containing either a control shRNA or *Fos* shRNA that were subsequently depolarized for 0, 1, 3 or 6 h with KCl treatment. We then assessed the effect of reducing FOS protein levels on the expression of individual activity-regulated genes. Western blot analysis of protein lysates obtained from paired cortical cultures demonstrated that *Fos* shRNA blocked the induction of FOS protein nearly completely at each time point of KCl stimulation examined (**Fig. 6a**). Notably, the induction of FOSB and the levels of several activity-dependent post-translational modifications (MEF2D dephosphorylation and CREB phosphorylation at Ser133) were unchanged, indicating that activity-regulated signaling overall was not affected by lentiviral infection and *Fos* shRNA expression (**Fig. 6a**).

To determine the effect of *Fos* knockdown on activity-regulated gene transcription, we focused our analysis on activity-regulated genes (genes in control shRNA–infected cultures that were upregulated at least threefold in response to KCl compared to the unstimulated condition; **Fig. 6b**) and compared their induction between the control shRNA and *Fos* shRNA conditions. *Fos* shRNA reduced the induction of 187/376 activity-regulated genes by at least 33%, suggesting that FOS is important for the proper transcriptional activation of a substantial fraction of the activity-regulated gene program in cortical neurons (**Supplementary Table 2**). To determine which of these putative FOS target genes are directly regulated by FOS, we determined which of the activity-regulated genes that are downregulated by *Fos* shRNA also have a FOS ChIP-seq peak located nearby (within 100 kb of the TSS) that exhibits activity-regulated enhancer features (CBP/H3K4me1 enrichment or increasing H3K27ac in response to neuronal activity). For this purpose, we considered all CBP/H3K4me1-enriched enhancers that have an increase in H3K27ac rather than including only enhancers that exhibit the largest fold increases (i.e., the previously defined increasing H3K27ac group). Of the 187 putative FOS target genes, 53 met these criteria (**Supplementary Table 2**). These data suggest that a substantial fraction of the genes misregulated by FOS knockdown are likely direct FOS targets. However, it is important to note that loss of FOS function can be partly compensated for by FOSB, as well as more distantly related AP-1 family members such as FOSL1 and FOSL2 (ref. 32). Therefore, it is possible that the identification of direct targets of FOS using the criteria described above might underestimate the number of enhancers that require AP-1 heterodimer binding for their function. This idea is consistent with the results of the AP-1 loss-of-function luciferase reporter assays (**Fig. 5a**,**b**) that demonstrated more marked effects on reporter expression when the AP-1 motif was mutated compared to co-transfection with *Fos* shRNA.

Among the direct FOS targets were genes known to be important for activity-regulated processes in neurons, including the postsynaptic scaffolding protein GRASP that has been shown to regulate metabotropic glutamate receptors[33], the secreted protein NPTX2 that regulates AMPA receptor clustering, homeostatic scaling and critical-period plasticity[7,34,35], the hormone IGF1 that has been shown to be important for brain development[36] and the histone deacetylase HDAC9 that is highly expressed within the nervous system and is thought to regulate dendrite development (**Fig. 7**)[37]. Notably, the majority of these direct FOS target genes (10/14) were effectively induced in the cortex after exposure of dark-reared mice to light (**Fig. 8**). This finding indicates that these FOS targets also mediate the effects of sensory stimuli in the intact brain.

Taken together, these findings suggest that sensory stimuli that induce *Fos* in the brain trigger FOS binding to thousands of enhancer sequences across the genome, and through a subset of these enhancers (for example, the enhancers that are enriched for CBP/H3K4me1 and exhibit increasing H3K27ac in response to neuronal activity), FOS induces changes in gene expression that underlie the neuronal response to sensory stimuli.

DISCUSSION

In this study, we identified a dynamic chromatin signature that enables the comprehensive mapping of the enhancers that promote activity-regulated transcription in cortical neurons. Although previous work had identified ~12,000 putative neuronal activity–regulated enhancers on the basis of CBP/H3K4me1 enrichment, we demonstrate that only the subset of these sites that is rapidly acetylated at H3K27 in response to neuronal activity can drive activity-regulated transcription. Having identified these functional *cis*-regulatory sites, we demonstrate that a common feature of many of these enhancers is their ability to bind the activity-induced transcription factor FOS. The induction of *Fos* in response to membrane depolarization is critical for activity-dependent enhancer function and for activation of a large subset of the genes that comprise the neuronal activity–regulated gene program. These findings suggest a pervasive and previously unappreciated function for FOS at neuronal activity–regulated enhancers.

In recent years, the ability to comprehensively identify the enhancers that are active in a given cellular state has provided important insight into the transcriptional regulatory events that govern cell fate specification during development. However, it was not known whether stimulus-responsive enhancers would exhibit the same features as constitutively active enhancers. Thus, identification of a chromatin signature that marks specifically the subset of cellular enhancers that control neuronal activity–dependent gene expression (increased H3K27ac in response to membrane depolarization) is an important step toward characterizing the mechanism of action and biological functions of stimulus-responsive enhancers.

Despite its widespread use in enhancer identification, the function of H3K27ac and its regulation by histone acetyltransferases and histone deacetylases are not well characterized[24]. H3K27ac is thought

to be catalyzed by CBP, a histone acetyltransferase and transcriptional coactivator that binds to as many as 12,000 enhancers when neurons are exposed to a depolarizing stimulus[18]. However, our data indicate that only a small fraction (1,468/11,830, 12.4%) of these CBP-bound enhancers exhibit activity-induced increases in H3K27ac, suggesting that recruitment of CBP to an enhancer in response to neuronal activity is not sufficient to initiate H3K27ac. Taken together with several recent studies in other cell types, our findings suggest that there are likely to be additional factors that regulate the acetyltransferase activity of CBP (and the highly related histone acetyltransferase p300) once it is bound to enhancers[22,23]. Furthermore, we provide evidence that sites with increasing H3K27ac but without detectable CBP/H3K4me1 enrichment function as enhancers in the context of native chromatin (but not in luciferase reporter assays). It will be important to determine whether this is the result of differences in the sensitivity of detection of CBP binding compared to H3K27ac. If the sensitivity of CBP detection by ChIP-seq is low, it could be difficult to detect CBP binding at enhancers with observable changes in H3K27ac that are bound by CBP only in a specific subset of neurons present in the mixed cortical cultures. As ChIP-seq techniques mature, it should be possible to investigate enhancer function in specific neuronal cell types, which will be required to investigate these issues further. In neurons, CBP binding is largely activity regulated, as we detected relatively few CBP binding sites (~1,000) before membrane depolarization. Given the importance of CBP in Rubinstein-Taybi syndrome, as well as increasing evidence that HDACs are critical mediators of activity-regulated transcription and are mutated in human disorders of cognitive function, it will be important to characterize the specific functions of these histone-modifying complexes at activity-regulated enhancers in neurons[38].

The comprehensive identification of the enhancers that promote activity-dependent gene transcription in cultured cortical neurons is a first step in understanding how this class of enhancers functions to initiate and/or amplify gene transcription in the brain during learning, memory and behavior. It is likely that the activity-dependent enhancers that we identified in cultured neurons function in a similar manner in the brain in response to sensory stimuli given that these regulatory elements are DNaseI hypersensitive and enriched for H3K27ac in the brain and the genes these enhancers regulate are induced in the cortex of dark-reared mice that have been exposed to light. However, the importance of FOS at activity-dependent enhancers *in vivo* remains to be established. Our efforts to detect FOS binding by ChIP–quantitative PCR (qPCR) at activity-regulated enhancers in brain extracts from mice that were dark reared and exposed to light have so far been unsuccessful. This outcome may reflect the increased heterogeneity of neurons in the intact cortex and possibly the fact that activity-dependent enhancers function in a cell type–specific manner, resulting in a much larger repertoire of FOS-bound enhancers *in vivo* that are difficult to detect in a heterogeneous population of neurons.

Although early response transcription factors such as FOS are thought to be critical for stimulus-responsive transcription in virtually all cell types in the body, our understanding of how these transcription factors activate transcription of their target genes in a cell type–specific manner is incomplete. In the nervous system, transcription of early response genes encoding transcription factors, including *Fos*, *Fosb*, *Junb*, *Nr4a1*, *Egr1* and *Npas4*, has been used to mark neurons that are activated by sensory input, and the induction of these transcription factors is thought to be required for the proper activation of late-response genes, which include critical regulators of dendrite development, synaptic maturation and circuit plasticity. By mapping the binding sites of the AP-1 transcription factors FOS, FOSB and JUNB in membrane-depolarized cortical neurons, we discovered that the vast majority of binding sites for these factors are located far away from the start sites for gene transcription. The extreme preference of AP-1 transcription factors for binding to enhancers suggests that FOS-JUN heterodimers may function in a unique manner at enhancers that is specifically tailored to enhancer function and is different from the mechanism by which transcription factors function at promoters. Further studies of FOS may provide new insight into how transcription factors bound to enhancers are capable of promoting transcription by acting from a location that is far from the site of transcriptional initiation.

The identification of FOS-bound enhancers in cortical neurons has allowed us to identify over 50 direct FOS target genes in these cells. These FOS target genes include well-characterized regulators of synaptic development and plasticity such as *Nptx2*, *Igf1*, *Grasp* and *Hdac9*, indicating that even though *Fos* can be induced in essentially all mammalian cell types, FOS activates targets in neurons that have neuronal-specific functions. It will be interesting to determine how these FOS targets are specified during neural development. Given the diversity of cell types in the nervous system, it seems likely that the functional activity–regulated enhancers, as well as FOS-bound enhancers, will also be found to differ from one neuronal cell type to another. It will be useful in the future to define the range of FOS-bound, activity-regulated enhancers in different types of neurons, as this information has the potential to reveal in greater depth how sensory inputs through FOS specify neuronal responses in the developing and mature nervous system.

METHODS

Methods and any associated references are available in the online version of the paper.

Accession codes. The ChIP-seq data generated in this study, including relevant processed data files, have been deposited in Gene Expression Omnibus (GEO) under accession number GSE60192. The microarray gene expression data generated in this study, including relevant processed data files, have been deposited in GEO under accession number GSE60049. Additional data used in this manuscript are deposited in GEO under accession numbers GSE21161, GSE52386, GSM1264352 (forebrain E11.5 H3K27ac Rep1), GSM1264354 (forebrain E11.5 H3K27ac Rep2), GSM1264356 (forebrain E14.5 H3K27ac), GSM1264358 (forebrain E17.5 H3K27ac), GSM1264360 (forebrain P0 H3K27ac), GSM1264362 (forebrain P7 H3K27ac), GSM1264364 (forebrain P21 H3K27ac), GSM1264366 (forebrain P56 H3K27ac Rep1) and GSM1264368 (forebrain P56 H3K27ac Rep2).

Note: Any Supplementary Information and Source Data files are available in the online version of the paper.

ACKNOWLEDGMENTS

We thank all the members of M.E.G.'s lab for their scientific support and helpful discussions. This work was funded by the US National Institutes of Health (NIH project 5R37NS028829-25 to M.E.G.), the National Institute of General Medical Sciences award number T32GM007753 (A.N.M.) and National Cancer Institute Institutional Training grant T32CA009361 (T.V.). T.V. and H.S. are both Howard Hughes Medical Institute Fellows of the Damon Runyon Cancer Research Foundation. E.L. is supported by the National Science Foundation Graduate Research Fellowship under grant numbers DGE0946799 and DGE1144152. The content of this study is solely the responsibility of the authors and does not necessarily represent the official views of the funding sources mentioned.

AUTHOR CONTRIBUTIONS

A.N.M. and M.E.G. conceived the study. A.N.M. performed experiments with assistance from T.V., A.A.R., E.L., I.S. and C.H.C. A.N.M. performed analysis of

microarray experiments. A.N.M. performed analysis of genome-wide sequencing experiments with assistance from M.H., H.S., K.K.-H.F. and D.A.H. A.N.M. generated figures with assistance from T.V. T.V., A.N.M. and M.E.G. wrote the manuscript.

COMPETING FINANCIAL INTERESTS

The authors declare no competing financial interests.

1. Greer, P.L. & Greenberg, M.E. From synapse to nucleus: calcium-dependent gene transcription in the control of synapse development and function. *Neuron* **59**, 846–860 (2008).
2. Leslie, J.H. & Nedivi, E. Activity-regulated genes as mediators of neural circuit plasticity. *Prog. Neurobiol.* **94**, 223–237 (2011).
3. Hensch, T.K. Critical period plasticity in local cortical circuits. *Nat. Rev. Neurosci.* **6**, 877–888 (2005).
4. Alberini, C.M. Transcription factors in long-term memory and synaptic plasticity. *Physiol. Rev.* **89**, 121–145 (2009).
5. Day, J.J. & Sweatt, J.D. Epigenetic mechanisms in cognition. *Neuron* **70**, 813–829 (2011).
6. Lyons, M.R. & West, A.E. Mechanisms of specificity in neuronal activity-regulated gene transcription. *Prog. Neurobiol.* **94**, 259–295 (2011).
7. O'Brien, R.J. *et al.* Synaptic clustering of AMPA receptors by the extracellular immediate-early gene product Narp. *Neuron* **23**, 309–323 (1999).
8. Hong, E.J., McCord, A.E. & Greenberg, M.E. A biological function for the neuronal activity-dependent component of Bdnf transcription in the development of cortical inhibition. *Neuron* **60**, 610–624 (2008).
9. Lin, Y. *et al.* Activity-dependent regulation of inhibitory synapse development by Npas4. *Nature* **455**, 1198–1204 (2008).
10. Ebert, D.H. & Greenberg, M.E. Activity-dependent neuronal signalling and autism spectrum disorder. *Nature* **493**, 327–337 (2013).
11. Greenberg, M.E. & Ziff, E.B. Stimulation of 3T3 cells induces transcription of the c-fos proto-oncogene. *Nature* **311**, 433–438 (1984).
12. Greenberg, M.E., Ziff, E.B. & Greene, L.A. Stimulation of neuronal acetylcholine receptors induces rapid gene transcription. *Science* **234**, 80–83 (1986).
13. Eferl, R. & Wagner, E.F. AP-1: a double-edged sword in tumorigenesis. *Nat. Rev. Cancer* **3**, 859–868 (2003).
14. Banerji, J., Rusconi, S. & Schaffner, W. Expression of a β-globin gene is enhanced by remote SV40 DNA sequences. *Cell* **27**, 299–308 (1981).
15. Levine, M. Transcriptional enhancers in animal development and evolution. *Curr. Biol.* **20**, R754–R763 (2010).
16. Heintzman, N.D. *et al.* Distinct and predictive chromatin signatures of transcriptional promoters and enhancers in the human genome. *Nat. Genet.* **39**, 311–318 (2007).
17. Visel, A. *et al.* ChIP-seq accurately predicts tissue-specific activity of enhancers. *Nature* **457**, 854–858 (2009).
18. Kim, T.K. *et al.* Widespread transcription at neuronal activity-regulated enhancers. *Nature* **465**, 182–187 (2010).
19. Maurano, M.T. *et al.* Systematic localization of common disease-associated variation in regulatory DNA. *Science* **337**, 1190–1195 (2012).
20. Visel, A. *et al.* A high-resolution enhancer atlas of the developing telencephalon. *Cell* **152**, 895–908 (2013).
21. Telese, F., Gamliel, A., Skowronska-Krawczyk, D., Garcia-Bassets, I. & Rosenfeld, M.G. "Seq-ing" insights into the epigenetics of neuronal gene regulation. *Neuron* **77**, 606–623 (2013).
22. Creyghton, M.P. *et al.* Histone H3K27ac separates active from poised enhancers and predicts developmental state. *Proc. Natl. Acad. Sci. USA* **107**, 21931–21936 (2010).
23. Rada-Iglesias, A. *et al.* A unique chromatin signature uncovers early developmental enhancers in humans. *Nature* **470**, 279–283 (2011).
24. Calo, E. & Wysocka, J. Modification of enhancer chromatin: what, how, and why? *Mol. Cell* **49**, 825–837 (2013).
25. Hsu, Y.C. & Perin, M.S. Human neuronal pentraxin II (NPTX2): conservation, genomic structure, and chromosomal localization. *Genomics* **28**, 220–227 (1995).
26. Shen, Y. *et al.* A map of the *cis*-regulatory sequences in the mouse genome. *Nature* **488**, 116–120 (2012).
27. Mouse ENCODE Consortium. *et al.* An encyclopedia of mouse DNA elements (Mouse ENCODE). *Genome Biol.* **13**, 418 (2012).
28. Crawford, G.E. *et al.* Genome-wide mapping of DNase hypersensitive sites using massively parallel signature sequencing (MPSS). *Genome Res.* **16**, 123–131 (2006).
29. Nord, A.S. *et al.* Rapid and pervasive changes in genome-wide enhancer usage during mammalian development. *Cell* **155**, 1521–1531 (2013).
30. Bailey, T.L. *et al.* MEME SUITE: tools for motif discovery and searching. *Nucleic Acids Res.* **37**, W202–W208 (2009).
31. Gerstein, M.B. *et al.* Architecture of the human regulatory network derived from ENCODE data. *Nature* **489**, 91–100 (2012).
32. Fleischmann, A. *et al.* Fra-1 replaces c-Fos–dependent functions in mice. *Genes Dev.* **14**, 2695–2700 (2000).
33. Kitano, J. *et al.* Tamalin, a PDZ domain–containing protein, links a protein complex formation of group 1 metabotropic glutamate receptors and the guanine nucleotide exchange factor cytohesins. *J. Neurosci.* **22**, 1280–1289 (2002).
34. Gu, Y. *et al.* Obligatory role for the immediate early gene NARP in critical period plasticity. *Neuron* **79**, 335–346 (2013).
35. Chang, M.C. *et al.* Narp regulates homeostatic scaling of excitatory synapses on parvalbumin-expressing interneurons. *Nat. Neurosci.* **13**, 1090–1097 (2010).
36. Beck, K.D., Powell-Braxton, L., Widmer, H.R., Valverde, J. & Hefti, F. Igf1 gene disruption results in reduced brain size, CNS hypomyelination, and loss of hippocampal granule and striatal parvalbumin-containing neurons. *Neuron* **14**, 717–730 (1995).
37. Sugo, N. *et al.* Nucleocytoplasmic translocation of HDAC9 regulates gene expression and dendritic growth in developing cortical neurons. *Eur. J. Neurosci.* **31**, 1521–1532 (2010).
38. Ronan, J.L., Wu, W. & Crabtree, G.R. From neural development to cognition: unexpected roles for chromatin. *Nat. Rev. Genet.* **14**, 347–359 (2013).

ONLINE METHODS

Mouse cortical neuron culture. E16.5 C57BL/6 embryonic mouse cortices were dissected and then dissociated for 10 min in 1× Hank's balanced salt solution (HBSS) containing 20 mg/mL trypsin (Worthington Biochemicals) and 0.32 mg/mL L-cysteine (Sigma). Trypsin treatment was terminated by washing dissociated cells three times for 2 min each in dissociation medium consisting of 1× HBSS containing 10 mg/mL trypsin inhibitor (Sigma). Cells were then triturated using a flame-narrowed Pasteur pipette to fully dissociate cells. After dissociation, neurons in were kept on ice in dissociation medium until plating. Cell culture plates were precoated overnight with a solution containing 20 µg/mL poly-D-lysine (Sigma) and 4 µg/mL mouse laminin (Invitrogen) in water. Prior to plating neurons, cell culture plates were washed three times with sterile distilled water and washed once with Neurobasal medium (Life Technologies). Neurons were grown in neuronal medium consisting of Neurobasal medium containing B27 supplement (2%; Invitrogen), penicillin-streptomycin (50 g/mL penicillin and 50 U/mL streptomycin; Sigma) and glutamine (1 mM; Sigma). At the time of plating, cold neuronal medium was added to neurons in dissociation medium to dilute neurons to the desired concentration. Neurons were subsequently plated and placed in a cell culture incubator that maintained a temperature of 37 °C and a CO_2 concentration of 5%. Two hours after plating neurons, the medium was completely aspirated from cells and replaced with fresh warm neuronal medium. Neurons were grown *in vitro* until DIV7. For ChIP-seq experiments, mouse cortical neurons were plated at an approximate density of 4×10^7 on 15-cm dishes. Neurons were plated in 30 mL neuronal medium. Ten milliliters of the medium was replaced with 12 ml fresh warm medium on DIV3 and DIV6.

For luciferase reporter assays, mouse cortical neurons were plated at an approximate density of 3×10^5 per well on 24-well plates. Neurons were plated in 500 µL neuronal medium. On DIV3, 100 µL fresh warm medium was added to neurons. On DIV5, neurons were transfected (more details are listed in the section on transfection). At the completion of transfection, conditioned medium containing 15% fresh medium was returned to the neurons.

Stimulation with potassium chloride. Prior to KCl depolarization, neurons were silenced with 1 µM tetrodotoxin (TTX; Fisher) and 100 µM DL-2-amino-5-phosphopentanoic acid (DL-AP5; Fisher). Neurons were subsequently stimulated by adding warmed KCl depolarization buffer (170 mM KCl, 2 mM $CaCl_2$, 1 mM $MgCl_2$ and 10 mM 4-(2-hydroxyethyl)-1-piperazineethanesulfonic acid (HEPES)) directly to the neuronal culture to a final concentration of 31% in the neuronal culture medium within the culture plate or well. For KCl depolarization of neurons for ChIP-seq experiments, DIV6 neurons were silenced overnight with 1 µM TTX and 100 µM DL-AP5. The next morning, neurons were left silenced (– KCl condition) or stimulated for 2 h with KCl (+ KCl condition). For KCl depolarization of neurons for luciferase reporter assays, DIV7 neurons were silenced for 2 h with 1 µM TTX and 100 µM DL-AP5. Two hours later, neurons were left silenced (– KCl condition) or stimulated for 6 h with KCl (+ KCl condition).

ChIP-seq. 40 million mouse cortical neurons cultured to DIV7 were used for each ChIP-seq library construction. Typically, 20–40 million cortical neurons were used for a single ChIP experiment. To crosslink protein–DNA complexes, the medium was removed from neuronal cultures, and crosslinking buffer (0.1 M NaCl, 1 mM ethylenediaminetetraacetic acid (EDTA), 0.5 mM ethylene glycol tetraacetic acid (EGTA) and 25 mM HEPES-KOH, pH 8.0) containing 1% formaldehyde was added for 10 min at room temperature (RT). Crosslinking was quenched by adding 125 mM glycine for 5 min at RT. Cells were then rinsed three times in ice-cold PBS containing complete protease inhibitor cocktail tablets (Roche) and collected by scraping. Cells were pelleted and either stored at –80 °C until use or processed immediately. Cell pellets were lysed by 20 cell pellet volumes (CPVs) of buffer 1 (50 mM HEPES-KOH, pH 7.5, 140 mM NaCl, 1 mM EDTA, pH 8.0, 10% glycerol, 0.5% NP-40, 0.25% Triton X-100 and complete protease inhibitor cocktail) for 10 min at 4 °C. Nuclei were then pelleted by centrifugation at 3,000 r.p.m. for 10 min at 4 °C. The isolated nuclei were rinsed with 20 CPVs of buffer 2 (200 mM NaCl, 1 mM EDTA, pH 8.0, 0.5 mM EGTA, pH 8.0, 10 mM Tris-HCl, pH 8.0, and complete protease inhibitor cocktail) for 10 min at RT and re-pelleted. Next, 4 CPVs of buffer 3 (1 mM EDTA, pH 8.0, 0.5 mM EGTA, pH 8.0, 10 mM Tris-HCl, pH 8.0, and complete protease inhibitor cocktail) were added to the nuclei, and sonication was carried out using a Misonix 3000 Sonicator (Misonix) set at a power setting of 7.5 (equivalent to 24 W). 20 pulses of 15 s each were delivered at this setting, which resulted in genomic DNA fragments with sizes ranging from 200 bp to 2 kb. Insoluble materials were removed by centrifugation at 20,000 r.p.m. for 10 min at 4 °C. The supernatant was transferred to a new tube, and the final volume of the resulting nuclear lysate was adjusted to 1 mL by adding buffer 3 supplemented with 0.3 M NaCl, 1% Triton X-100 and 0.1% deoxycholate. The lysate was precleared by adding 100 µL of pre-rinsed Protein A/G Agarose (Sigma) per 1 ml of the lysate and incubating for 1 h at 4 °C. After preclearing, 10% of the ChIP sample (50 µL from 500 µL lysate) was saved as input material. The remaining lysate was incubated with antibodies for immunoprecipitation. The antibody incubation was carried out overnight at 4 °C. The next day, 30 µL of pre-rinsed Protein A/G PLUS Agarose beads (Santa Cruz Biotechnology) was added to each ChIP reaction and further incubated for 1 h at 4 °C. The beads bound by immune complexes were pelleted and washed twice with each of the following buffers: low-salt buffer (0.1% SDS, 1% Triton X-100, 2 mM EDTA, 20 mM Tris-HCl, pH 8.1, and 150 mM NaCl), high-salt buffer (0.1% SDS, 1% Triton X-100, 2 mM EDTA, 20 mM Tris-HCl, pH 8.1, and 500 mM NaCl) and LiCl buffer (0.25 M LiCl, 1% IGEPAL CA630, 1% deoxycholic acid (sodium salt), 1 mM EDTA and 10 mM Tris, pH 8.1). In each wash, the beads were incubated with wash buffer for 10 min at 4 °C while nutating. The washed beads were then rinsed once with 1× TE buffer (10 mM Tris-HCl, pH 8.0, and 1 mM EDTA). The immunoprecipitated material was eluted from the beads twice by adding 100 µL of elution buffer (10 mM Tris-HCl, pH 8.0, 1 mM EDTA, pH 8.0, and 1% SDS) to each ChIP reaction and incubating the sample at 65 °C for 30 min with brief vortexing every 2 min. 150 µL of elution buffer was also added to the saved input material (50 µL), and this sample was processed together with the ChIP samples. The eluates were combined, and crosslinking was reversed by incubation at 65 °C overnight. The next day, 7 µg RNase A (affinity purified, 1 mg/mL; Invitrogen) was added to each sample, and samples were incubated at 37 °C for 1 h. Then, 7 µL Proteinase K (RNA grade, 20 mg/mL; Invitrogen) was added to each sample, and samples were incubated at 55 °C for 2 h. The immunoprecipitated genomic DNA fragments were then extracted once with phenol:chloroform:isoamyl alcohol (25:24:1, pH 7.9; Life Technologies) and then back extracted with water. The resulting genomic DNA fragments were then purified using the QIAquick PCR purification kit (Qiagen), and DNA fragments were eluted in 100 µl of buffer EB (elution buffer consisting of 10 mM Tris-HCl, pH 8.5; Qiagen). Samples were assessed for enrichment by qPCR using primers to different genomic regions. Samples with significant enrichment over negative regions were submitted to the Beijing Genomic Institute (BGI) for 50-bp single-end sequencing on the Illumina HiSeq 2000 platform. For each sample, over 20 million clean reads were obtained.

Antibodies. Antibodies to the following were used: H3K27ac (Abcam, ab4729, 0.5 µg/ChIP), FOS (Santa Cruz, sc-52, 4 µg/ChIP, primary antibody used for ChIP-seq), FOS (Santa Cruz, sc-7202, 4 µg/ChIP, used for an additional ChIP-seq replicate and for western blotting for FOS; **Figs. 4b** and **6a** and **Supplementary Fig. 5a**), FOSB (Santa Cruz, sc-48, 4 µg/ChIP), JUNB (Santa Cruz, sc-46, 4 µg/ChIP), pCREB (Ser133) (Millipore, clone 10E9), MEF2D (BD Biosciences; Cat. No. 610774) and MECP2-p421 (generated in M.E.G.'s laboratory[39]). For western blot analysis, antibodies were used at a 1:1,000 dilution with goat anti-mouse and goat anti-rabbit horseradish peroxidase (HRP)-conjugated secondary antibodies (115-035-003 and 111-035-003) used at a 1:20,000 dilution.

ChIP-seq analysis. Sequencing data were obtained from BGI in gzipped fastq file format. Files were transferred and unzipped. Then sequencing reads were aligned to the July 2007 assembly of the mouse genome (NCBI 37, mm9) using the Burrows-Wheeler Aligner (BWA) with default settings[40]. The resulting bwa files were then converted to sam files, and uniquely mapped reads were extracted from the sam files. Sam files of the uniquely mapped reads were then converted to bam files. Bam files were then used for peak calling using model-based analysis of ChIP-seq (MACS)[41] with the following parameters: -f BAM -g mm–nomodel–shiftsize = 150. To visualize ChIP-seq data on the UCSC genome browser, ChIP-seq bam files were converted to bigwig track format to display the number of input-normalized ChIP-Seq reads normalized to 20 million total reads.

H3K27ac peaks were classified on the basis of their location relative to genes in the NCBI Reference Sequence Database (RefSeq). H3K27ac peaks were classified as being proximal if they were within 1 kb of an annotated TSS. H3K27ac peaks

doi:10.1038/nn.3808

were classified as being distal if they were greater than 1 kb from an annotated TSS. Distal H3K27ac peaks were further classified as intragenic if they occurred within a RefSeq gene or as extragenic if they did not occur within a RefSeq gene. For chromatin modifications (H3K4me1 and H3K27ac), the number of input-normalized ChIP-seq reads within a 2-kb window centered on each enhancer was taken to be the ChIP-seq signal at the enhancer. For transcription factors (CBP), the number of input-normalized ChIP-seq reads within an 800-bp window centered on each enhancer was taken to be the ChIP-seq signal at the enhancer. Quantifications of ChIP-seq and RNA-seq data relating to the CBP/H3K4me1-enriched enhancers identified in Kim *et al.*[18] are supplied in **Supplementary Table 3**.

Enhancers were classified into different categories on the basis of the behavior of the quantified H3K27ac signal at each enhancer. Enhancers were classified as having increasing H3K27ac if they exhibited a twofold or greater increase in H3K27ac signal with stimulation and if the stimulated signal for H3K27ac was not within the bottom quartile of H3K27ac signals at all enhancers identified in the stimulated condition. Enhancers were classified as having decreasing H3K27ac if they exhibited a 50% or greater decrease in H3K27ac signal with stimulation and if the unstimulated signal for H3K27ac was not within the bottom quartile of H3K27ac signals at all enhancers identified in the unstimulated condition. Enhancers were classified as having constant H3K27ac if they exhibited H3K27ac signal in the top quartile of all enhancers identified in both the unstimulated and stimulated conditions and if the H3K27ac signal changed by 10% or less with stimulation. Enhancers were classified as having no H3K27ac if they were identified previously on the basis of inducible CBP binding and enrichment for H3K4me1 (ref. 18) but did not overlap with H3K27ac peaks within the H3K27ac data sets generated in this study.

For FOS ChIP-seq, three biological replicates were performed from paired membrane-depolarized and unstimulated neuronal cultures using an antibody to FOS (sc-52, Santa Cruz Biotechnology), and two of these three replicates included an additional paired sample of neurons infected with FOS shRNA lentivirus in pLL3.7 (to confirm the specificity of this antibody). MACS identified 19,077 peaks called over the input chromatin (using default threshold parameters, MACS $P = 1 \times 10^{-5}$) that were reproducibly detected in 2/3 biological replicates. Of these sites, the ChIP-seq signals at 12,594 were reduced by least 50% in 2/2 shRNA experiments. We focused on this set of reproducible and specific FOS peaks for subsequent analysis. In addition, we performed one further replicate of FOS ChIP-seq with a second antibody to FOS (sc-7202, Santa Cruz Biotechnology) to further confirm the specificity of these peaks (**Fig. 3b** and **Supplementary Fig. 3a**).

RNA-seq analysis. RNA-seq data from a previous study[18] were analyzed and integrated into this study. For nearest-gene analyses, the nearest gene (with nonzero expression) to an enhancer was linked to that enhancer, and the expression of the genes nearest to each class of enhancers was characterized.

Neuronal transfection. Mouse cortical neurons plated on 24-well plates at a density of approximately 3×10^5 neurons per well were transfected for luciferase reporter assays using Lipofectamine 2000 reagent (Invitrogen) according to the manufacturer's protocol with slight modifications. Briefly, DNA mixes were made immediately preceding the transfection consisting of 1 µg total plasmid DNA per well diluted in Neurobasal medium (Life Technologies). DNA typically consisted of 450 ng firefly luciferase reporter DNA, 50 ng pGL4.74 *Renilla* luciferase reporter DNA (Promega) and 500 ng empty pCS2 plasmid[42] as filler DNA. Lipofectamine was used at 2 µL per well and was diluted in Neurobasal medium just before the transfection. Within each experiment, all conditions were transfected in two to three independent wells for technical duplicates or triplicates, respectively. Thirty minutes before the addition of Lipofectamine to neurons, the culture medium was removed and replaced with warmed Neurobasal medium. At this time, neurons were returned to the incubator, and DNA mixes were added to diluted Lipofectamine in a dropwise manner. After 30 min of incubation, DNA-Lipofectamine mixes were added to neurons, again in a dropwise manner. The cells were left to incubate with the DNA-Lipofectamine mix for 2 h, after which the transfection medium was replaced with supplemented conditioned neuronal medium.

After stimulation, neurons were lysed using Passive Lysis Buffer (Dual-Luciferase Reporter Assay System, Promega). Lysates were then collected in microcentrifuge tubes and frozen at −20 °C. At the time of performing the luciferase assay, neuronal lysates were thawed, briefly vortexed and briefly spun down, and then 20 µL of each sample was added to one well of Costar White Polystyrene 96-well Assay Plates (Corning). The reagents to run the luciferase assay, Luciferase Assay Reagent II (LARII) and Stop & Glo Reagent (Dual-Luciferase Reporter Assay System, Promega), were aliquoted and thawed according to the manufacturer's protocol. The luciferase assay was performed using the Synergy 4 Hybrid Microplate Reader (BioTek) with 100 µL of LARII and Stop & Glo Reagent injected per well. Data were subsequently downloaded and analyzed using Microsoft Excel.

Using the Dual-Luciferase Reporter Assay System, we recorded firefly (FF) and *Renilla* (Ren) luminescence from each well. To correct for variations in transfection efficiency and cell lysate generation, the FF values were normalized to Ren luminescence within each well, generating a ratio of FF/Ren. The stimulus-dependent fold induction of each reporter plasmid was obtained by dividing the (+ stimulus) FF/Ren value by the (− stimulus) FF/Ren value. To isolate the induction due to the enhancer, the fold induction of an enhancer reporter was divided by the fold induction of the appropriate backbone into which the enhancer was cloned, giving fold induction relative to the backbone. Fold induction relative to the backbone is the value shown in all figures containing luciferase reporter data.

Luciferase reporter assays. Most of the luciferase reporter plasmids used were based on the *Nptx2* gene, and hence this reporter was termed the *Nptx2* reporter. To develop the *Nptx2* reporter, we cloned the 4,355-bp region upstream of the *Nptx2* coding sequence from C57BL/6 purified mouse genomic DNA between the NheI and EcoRV restriction sites within the multiple cloning site of the promoterless pGL4.11 reporter plasmid (Promega) using sequence-specific primers (forward primer: GCGCGCTAGCTTCCTGGCTTGTAGTGACCT, reverse primer: GCGCGATATCCTCGCTGACCTGTGTGCTCACTTCA). pGL4.11 was chosen as the host plasmid because it contains the luc2P reporter gene, which contains an hPEST protein destabilization sequence. We found that the luc2P reporter responded more quickly and with greater magnitude to stimuli than the luc2 reporters. Using PCR-driven overlap extension, the *Nptx2* reporter was then modified so that the 1,216-bp *Nptx2* upstream enhancer (located −3607 to −2391 relative to the start of the *Nptx2* coding sequence) was replaced with a multiple cloning site containing SbfI, PacI, PmeI and AscI restrictions sites[43]. The multiple cloning site was inserted into the *Nptx2* upstream regulatory region to create a modified Nptx2 reporter so that various enhancers could be easily cloned into this multiple cloning site. We verified that the modified *Nptx2* reporter in which the *Nptx2* enhancer had been cloned into the multiple cloning site had the same induction as the wild-type *Nptx2* reporter (data not shown). This suggested that the multiple cloning site did not affect the function of the reporter and that other enhancers could be similarly cloned into this multiple cloning site without adverse affects on enhancer function. The pGL4.11 Nued2 reporter construct is available through Addgene (plasmid #59744).

To test enhancer function in additional reporter contexts, we generated two additional reporter constructs by modifying pGL4.24 (Promega), a luciferase reporter containing a minimal TATA box–containing promoter but not containing any enhancer elements. To facilitate cloning of enhancers from the *Nptx2* reporter plasmid into this plasmid, we first modified this plasmid by adding a multiple cloning site containing SbfI, PacI, PmeI and AscI sites between the BamHI and SalI sites downstream of the firefly luciferase gene (pGL4.24_minP_MCS). We then further modified pGL4.24_minP_MCS by removing the minimal TATA box–containing promoter from this plasmid and replacing this promoter with an SV40 promoter from another Promega luciferase reporter, the pGL3-Promoter Vector. This cloning was achieved using BglII and NcoI restriction sites flanking both promoter regions. This resulted in the generation of a separate reporter construct, pGL4.24_SV40_MCS, with which enhancer activity could be assessed.

Enhancers with different H3K27ac behaviors were cloned between the SbfI and AscI sites within the multiple cloning site of the modified *Nptx2* reporter. Cloned enhancer regions varied in size but were approximately 1 kb in length. Enhancers cloned using this strategy and the primers used to amplify each enhancer from mouse genomic DNA are listed in **Supplementary Table 4**. For *Nptx2* reporter assays with FOS shRNA co-transfection, a scrambled version of an shRNA targeting *Npas4* in the pLL3.7 vector was used as the control[9].

Lentiviral infection of shRNA constructs. shRNA targeting *Fos* (target sequence: 5′-GCCTTTCCTACTACCATTC-′3) or a control hairpin targeting firefly luciferase (target sequence: CTTACGCTGAGTACTTCGA) was cloned into the pLL3.7 plasmid (Addgene Plasmid #11795). For lentiviral infections, neurons were cultured as described above. On DIV5, lentiviral supernatant was applied to cultures for 6 h with 6 μg/mL polybrene. At DIV7, neurons were silenced and stimulated with KCl as described for 0, 1, 3 or 6 h, and total RNA was purified using TRIzol and the RNeasy mini kit from Qiagen. 10 μg of labeled cDNA was hybridized to Affymetrix mouse genome 430 2.0 arrays with Affymetrix processing. Microarray experiments were performed at the Dana Farber Microarray Core facility.

qRT-PCR of FOS direct target genes from the visual cortex. All experiments with mice were approved by the Animal Care and Use Committee of Harvard Medical School. For dark rearing, P49 C57BL/6J animals (two males and two females per condition) were placed into a dark chamber. At P56, animals were exposed to light for the indicated time periods. At the end of the light stimulus, visual cortices from each animal were removed and snap frozen in liquid nitrogen. For RNA extraction, the visual cortex from each animal was solubilized in 1 mL TRIzol, and RNA was extracted using the Qiagen RNeasy Mini kit according to the manufacturer's protocol. Complementary DNA was synthesized from 1 μg of input RNA using the ABI High Capacity cDNA synthesis kit with random primers. 5 ng of cDNA per reaction was used for qPCR reactions. Reactions were run in duplicate wells on a 384-well thermal cycler (Roche). The primers used are listed in **Supplementary Table 3**.

Correlation of defined motifs with H3K27ac dynamics. H3K27ac peaks were called based on windows at least 1,000 bp in size that contained an average of more than four genome-normalized reads per bp in the averaged before- and after-stimulation data. Peaks that were within 2,000 bp of a TSS were considered promoters, and the remainder of the peaks were classified as distal enhancer-like elements. The top motifs underlying both of these regions were identified using Homer[44]. Homer was also used to identify the fraction of FOS ChIP-seq peaks that contained an AP-1 motif.

Analysis of *in vivo* H3K27ac data. Data from ref. 29 were downloaded from GEO (GSE52386) and mapped to mm9 using bowtie allowing up to two mismatches and only retaining uniquely mapping reads. Reads mapping to identical locations were removed. Each data set was normalized to the total number of uniquely mapping reads.

A **Supplementary Methods Checklist** is available.

39. Zhou, Z. *et al.* Brain-specific phosphorylation of MeCP2 regulates activity-dependent Bdnf transcription, dendritic growth, and spine maturation. *Neuron* **52**, 255–269 (2006).
40. Li, H. & Durbin, R. Fast and accurate short read alignment with Burrows-Wheeler transform. *Bioinformatics* **25**, 1754–1760 (2009).
41. Zhang, Y. *et al.* Model-based analysis of ChIP-Seq (MACS). *Genome Biol.* **9**, R137 (2008).
42. Rupp, R.A., Snider, L. & Weintraub, H. *Xenopus* embryos regulate the nuclear localization of XMyoD. *Genes Dev.* **8**, 1311–1323 (1994).
43. Heckman, K.L. & Pease, L.R. Gene splicing and mutagenesis by PCR-driven overlap extension. *Nat. Protoc.* **2**, 924–932 (2007).
44. Heinz, S. *et al.* Simple combinations of lineage-determining transcription factors prime *cis*-regulatory elements required for macrophage and B cell identities. *Mol. Cell* **38**, 576–589 (2010).

doi:10.1038/nn.3808